Research Article Vol. 13, No. 10 / 1 Oct 2023 / *Optical Materials Express* 2737

Optical Materials EXPRESS

Characterization of the optical and electronic properties of chalcogenide hybrid inorganic/organic polymer thin films

STEPHANIE AROUH,[1,*] ABHINAV NISHANT,[1] JEFFREY PYUN,[2] AND ROBERT A. NORWOOD[1]

[1] *Wyant College of Optical Sciences, University of Arizona, Tucson 85721, AZ, USA*
[2] *Department of Chemistry and Biochemistry, College of Science, University of Arizona, Tucson, AZ 85721, USA*
[*] *rnorwood@optics.arizona.edu*

Abstract: Chalcogenide hybrid inorganic/organic polymers (CHIPs) are a new class of optical polymeric materials for imaging and photonic applications due to their high refractive indices and high optical transmission at visible and infrared wavelengths. In this study, we characterize these polymers to study the refractive index and delve into the electronic properties by way of measurements of their dielectric constants. Ellipsometry is used to determine the refractive indices for wavelengths from 500 nm to 12 µm, while we use capacitance measurements on thin film capacitors with a range of areas to find the dielectric constant. The results are in line with expectations based on the sulfur composition of the polymers-indices range from 1.7 to 1.85, and dielectric constants range from 2.6 to 3. With these measurements, these sulfur polymer materials are established to be good candidates for optical and photonic applications, particularly with respect to telecommunications. The dielectric constants suggest that applications such as electro-optic devices and capacitors may also be viable.

1. Introduction

Imaging at infrared wavelengths is an important aspect of many technologies, ranging from telecommunications at the near-IR, to thermal imaging, to 3-D sensing. Current IR materials such as GaAs, Ge, As_2Se_3, and chalcogenide glasses have good transmission at near and mid-IR wavelengths, and they have high refractive indices, but are expensive and difficult to work with as well as being difficult to manufacture on large scales. Optical polymers are convenient to process and are relatively low cost, but optical polymers generally are not highly transparent at IR wavelengths due to absorptive bond vibrations [1].

To overcome the difficulties, present with typical infrared (IR) materials and optical polymers, novel sulfur plastics have been explored. To reduce the IR absorption that is present due to atomic and molecular bond vibrations, heavier atoms are ideal. This is demonstrated with the standard mass and spring equations of motion that indicate that vibrations involving heavy atoms such as sulfur have reduced IR absorption in optical windows of interest in the infrared. Sulfur-based polymers are a type of novel chalcogenide polymer that are inexpensive, easily processed, and possess appreciable transparency at infrared wavelengths. The polymers are created by a process called inverse vulcanization [2], which involves breaking the bonds of elemental sulfur with heat and then reacting linear sulfur chains with small organic compounds to link together these molecules to create a copolymer. This method is simple and scalable, as demonstrated in previous work [3]. The polymer can be molded into lenses or other shapes [4], and can also be dissolved to create a solution that is used with the spin-coating method to create thin films for integrated photonics [5].

#499063
Journal © 2023

https://doi.org/10.1364/OME.499063
Received 27 Jun 2023; revised 16 Aug 2023; accepted 19 Aug 2023; published 8 Sep 2023

In this paper the first in depth study on the optical, and electronic properties of these new optical polymers is performed. Previously, the refractive indices have reported over a limited wavelength range [1,2], but this work aims to provide a more complete picture of the material properties for two important sulfur copolymers prepared by the inverse vulcanization process based on poly(sulfur-*random*-(1,3-diisopropenylbenzene) (poly(S-*r*-DIB) and (poly(sulfur-*random*-dimeric norbornadiene) (poly(S-*r*-NBD_2)). Ellipsometry is performed from visible wavelengths out to the long wave-IR for both S-*r*-DIB (50/50 and 70/30 wt% ratios) and S-*r*-NBD_2 (50/50 and 70/30 wt% ratios) CHIPs polymers; these complement IR absorption spectra that have been previously published [1,5]. The frequency dependent dielectric constant is also measured for poly(S-*r*-DIB) (both 50-wt% and 70-wt% sulfur compositions; as the dielectric constant measurement technique required a uniform thin film dielectric constant measurements were not performed on poly(S-*r*-NBD_2) as it is a thermoset and difficult to process into thin films. The results of the studies discussed herein further confirm that these sulfur derived polymers are suitable for optical applications such as lenses and optical waveguides; we also open up applications in the near- and mid-IR as well as electronic applications such as capacitors and printed circuit boards.

2. Materials and methods

2.1. Material synthesis

Poly(S-*r*-DIB) polymer is made by the inverse vulcanization process [2]. Elemental sulfur is heated above the melting point at 170°C and then mixed with 1,3-diisopropenylbenzene (DIB) in varying ratios to create poly(S-*r*-DIB). DIB is an ideal comonomer as it has high solubility in molten sulfur and readily reacts with linear sulfur chains allowing for a broad range of copolymer compositions to be synthesized. Poly(S-*r*-DIB) behaves like a thermoplastic polymer with a glass transition temperature in the range of 30-50°C, depending on composition. Since the polymer form formed from sulfur and DIB has both aliphatic and aromatic carbons, the infrared spectrum has numerous hydrocarbon vibrations. The material has excellent transparency in the mid-wave IR (MWIR; 3-5µm) compared to conventional polymers, but is essentially opaque in the long-wave IR (LWIR; 8-12µm).

Poly(S-*r*-NBD_2) is also made by the inverse vulcanization process, where in this case the comonomer is a dimer of norbornadiene [6]. Poly(S-*r*-NBD_2) was developed in response to the aforementioned shortcomings of S-*r*-DIB, namely low glass transition temperature and lack of transparency in the long-wave IR. Poly(S-*r*-NBD_2) behaves as a thermoset with a glass transition temperature of about 110°C; thus the material is more challenging to handle by solution processing methods to produce thin films. Furthermore, poly(S-*r*-NBD_2) polymer only has aliphatic carbons, which significantly simplifies the IR spectrum, leading to some transmission in the LWIR.

2.2. Material processing

Poly(S-*r*-DIB) polymer is dissolved in chlorobenzene, then the mixture is heated to 115°C while stirring continuously. Once the mixture is translucent red, it is removed from heat and cooled to room temperature. The mixture is then filtered with a 0.2µm filter into a new vial to remove impurities, particles, and any undissolved polymer.

Poly(S-*r*-DIB) copolymers (both 50-wt% and 70-wt% sulfur) were dissolved in hot chlorobenzene as described above at a ratio of 1 g S-DIB to 4 mL chlorobenzene. A silicon wafer was rinsed with acetone, DI water, and isopropyl alcohol, dried with N_2, then cleaned with oxygen plasma for 2-3 minutes. Approximately 1.0 mL of dissolved poly(S-*r*-DIB) copolymer is dropped onto the 1×1 inch^2 cleaned Si substrate, with a syringe using a 0.2µm filter, then spun at 1500 RPM to form thin films suitable for ellipsometry measurements. The silicon wafers were roughened on the bottom to prevent deleterious reflections.

Similar procedures were used to deposit thin films of poly(S-*r*-DIB) onto substrates of microscope glass coated with a thin (100 nm) layer of indium tin oxide (ITO) for dielectric constant measurements. On half of a 1 × 1 inch^2 glass/ITO substrate, the ITO is etched away with a wet etch using HCl:HNO_3:$5H_2O$. The ITO film is measured with a hand-held ohm-meter to monitor completion of the etch, where the completion of ITO etching was tracked by progression to essentially infinite sheet resistance. These thin film samples were only used for dielectric constant measurements and were not evaluated by ellipsometry.

Poly(S-*r*-NBD_2) thin film processing was achieved by casting of the monomers and curing into create relatively thick films (~ 1 mm thick), as is typical for a thermoset polymer. Bulk substrate mode ellipsometry was performed on these samples, whereas dielectric constant measurements were not attempted as thin film fabrication using this approach was not feasible.

The structures of the two polymers are shown in Fig. 1.

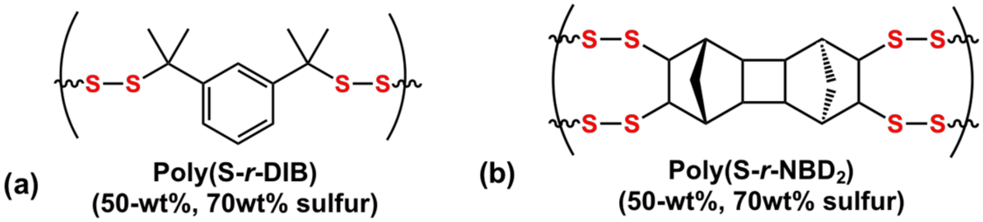

Fig. 1. Structures of the two materials studied (a) poly(S-*r*-DIB) and (b) poly(S-*r*-NBD_2).

3. Results

3.1. Refractive indices

3.1.1. Poly(S-*r*-DIB)

Ellipsometry was performed on thin films of sulfur copolymers on silicon wafer substrates using a Woolam M-2000 for the wavelength region from 193 nm to 1700 nm and a Woolam IR-VASE Mark II for the region from 1700 nm to 15 µm. Single-point measurements were performed at 25°C, using either two (60°, 70°) or four incident angles (55°, 60°, 65°, 70°). An uncoated silicon wafer reference was also measured and modeled using a Drude-Fano oscillator model with Woolam's CompleteEase software; the modeling determined the presence of a native oxide layer approximately 2 nm thick. For the reference silicon substrate, mean square error (MSE) in the 193 nm to 1700nm region were 5.2 while the MSE in the 1700nm to 15µm region was 1.7; MSE less than 10 is desired.

Typical psi-delta data is shown in Fig. 2 for the 50/50 poly (S-*r*-DIB), with fits accomplished using Woolam's CompleteEase software; the MSE for the data set was an acceptable value of 8.7. The psi-delta data was numerically inverted point-by-point and the resulting n and k data were then checked for physicality through the GenOsc routine of CompleteEase, which includes various oscillator models, Kramers-Kronig relationships, etc [7]. The film thicknesses were determined as part of the ellipsometric fitting and were found to be 1002.4 nm for the 50/50 poly (S-*r*-DIB) sample and 840.2 nm for the 70/30 poly (S-*r*-DIB) sample.

As can be seen in Fig. 3, there are multiple resonances in the refractive index spectrum that are due to atomic and molecular vibrations. Near 3.3-3.5µm there is a resonance due to the absorption caused by C-H and CH_3 (methyl group) bonds which is present in the IR spectra of many organic materials. Resonances are observed in the long wave-IR "fingerprint" region due

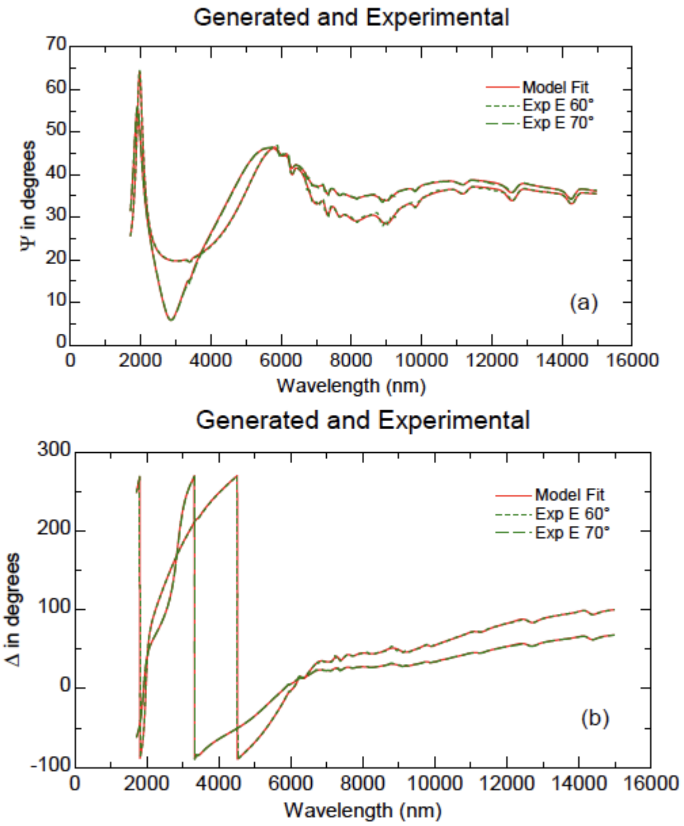

Fig. 2. Point-by-point numerical inversion fit to infrared ellipsometric psi(a) and delta(b) data for poly (S-*r*-DIB) 50/50 thin film sample on silicon

to numerous molecular vibrations present. These can be ascribed to the H-C-H bend (1333cm^{-1}), the CH methyl rock (1135cm^{-1}), the H-C-S bend (890cm^{-1}), the C-H bend (800cm^{-1}), and the C-S stretch (714cm^{-1}) respectively. Upon inspection of the refractive index over this extended wavelength range, we see that the optical dispersion for poly(S-*r*-DIB) materials exhibits low values in the NIR-SWIR from 1-3 µm and in the MWIR from 3.5-6 µm; indicating that these are regions where high performance broadband imaging is possible with optics made from these materials. This low dispersion despite the high refractive index derives fundamentally from the high polarizability of the sulfur atoms that comprise a substantial portion of the materials. For the NIR-SWIR region, we can define a SWIR Abbe number given by

$$V_{\mathrm{SWIR}} = \frac{n_{1310} - 1}{n_{980} - n_{1550}} \tag{1}$$

where n_{980}, n_{1310}, and n_{1550} are the refractive indices at wavelengths of 980 nm, 1310 nm and 1550 nm, respectively. Note that there is, to our knowledge, no standard SWIR Abbe number; we have used this definition since these are wavelengths that many SWIR systems are based on. Using this definition we find that V_{SWIR} is 156 for the 50/50 material and 137 for the 70/30 material; higher dispersion is observed for the higher sulfur content poly(S-r-DIB), principally due to the contribution of the color to the refractive index at 980 nm. Additional optical dispersion in this spectral window can be attributed to the organic moieties in the material (i.e., vibrational overtones) [8]. The SWIR Abbe number values for poly(S-r-DIB) are lower than those of classic optical polymers, such as, poly(methylmethacrylate (PMMA) with a value of 435 [9], or polycarbonate (PC) at 177 [10], which can directly be attributed to the aforementioned impact on the SWIR Abbe number from the refractive index at 980 nm, which is elevated in poly(S-*r*-DIB) due to its orange color, whereas common optical polymers are generally colorless.

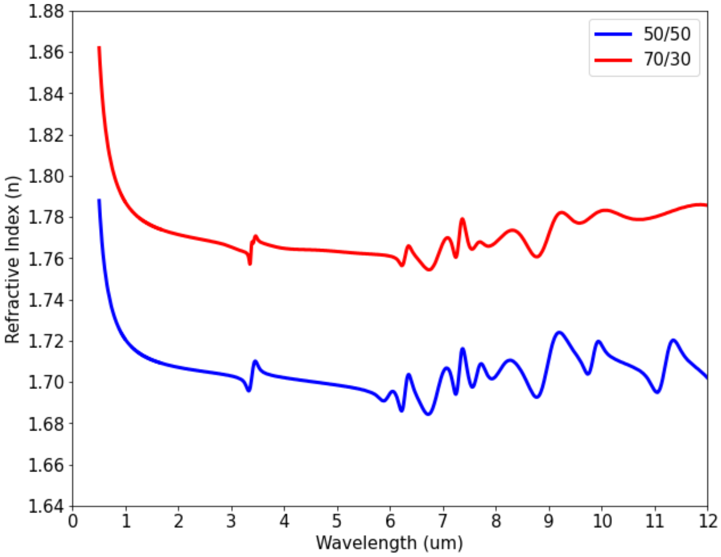

Fig. 3. Refractive indices (n) for thin films of poly(S-r-DIB) (50-wt% and 70-wt% sulfur) from 500 nm to 12 µm measured by spectroscopic ellipsometry in the thin film mode.

3.1.2. Poly(S-*r*-NBD$_2$)

Films were created using melt pressing of poly(S-*r*-NBD$_2$). Ellipsometric measurements were performed in the bulk substrate mode, which is generally less accurate than the thin film mode. In this case only one reflection (the air interface) is assumed - the bottoms of these samples were roughened to eliminate reflections from the backside. In this mode of operation, direct relationships exist between the ellipsometric parameters psi and delta data and n & k; these relationships were used to arrive at n & k in addition to using numerical inversion of the psi-delta data as mentioned above. The reduced accuracy of the bulk substrate mode results from the fact that there is information from only one interface, in addition to the lack of any internal propagation phase information. The refractive indices of poly(S-*r*-NBD$_2$) 50/50 and 70/30 are shown in Fig. 4. As in the case of poly(S-*r*-DIB), poly(S-*r*-NBD$_2$) evidences a strong resonance around 3.3-3.5µm that is due to C-H bonds. Note that the long wave IR around 10µm has much less structure than for poly(S-*r*-DIB). This is expected since the polymerized norbornadiene dimer has only C-C and C-H bonds with no aromatic C = C bonds present, greatly simplifying the spectrum in the LWIR. This leads to poly(S-*r*-NBD$_2$) having significantly higher transparency than poly(S-*r*-DIB) in the LWIR.

The SWIR Abbe numbers of poly(S-*r*-NBD$_2$) are 216 and 351 for the 50/50 and 70/30 compositions, respectively. These are both higher than the values for PC and the 70/30 composition approaches the V_{SWIR} value for PMMA; the increased SWIR Abbe numbers for poly(S-*r*-NBD$_2$) compared to poly(S-*r*-DIB) can be attributed primarily to the reduced color of poly(S-*r*-NBD$_2$), which is yellow as opposed to orange for poly(S-*r*-DIB), reducing the dispersion at 980 nm and thus increasing V_{SWIR}. It is remarkable that poly(S-*r*-NBD2), which is yellow, has a V_{SWIR} larger than PC and that the 70/30 formulation is nearly as high as PMMA. This derives

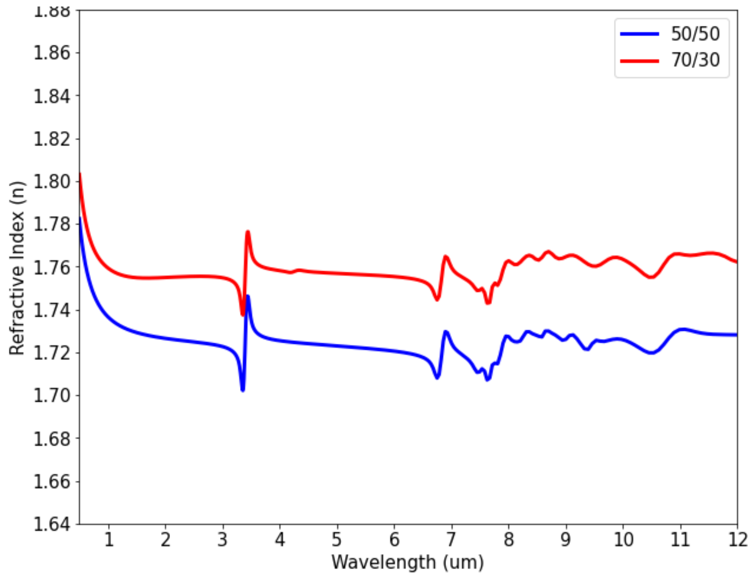

Fig. 4. Refractive indices for $SNBD_2$ with 50/50 and 70/30 ratios of sulfur to NBD2. Wavelength ranges from 500 nm to 12µm.

from the fact that the high refractive index of CHIPs materials principally comes from the high polarizability of the sulfur atom, with only a small amount of the refractive index coming from color (edge absorption); away from the absorption region, the dispersion of these polymers will decrease with increasing sulfur content, as is clearly seen for poly(S-*r*-NBD_2) even in the SWIR. The values for *k*, the imaginary part of the refractive index directly related to absorption, are low throughout the measured region of the IR for both polymer systems as shown in Fig. 5; note that the spectrum is much simpler for poly(S-*r*-NBD_2) owing to the norbornene monomer used in this material.

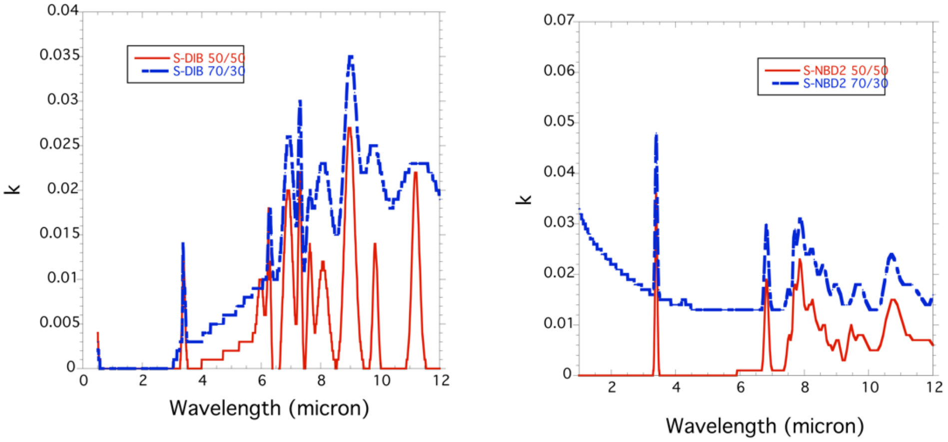

Fig. 5. Ellipsometric *k* values for poly(S-*r*-DIB) on the left and poly(S-*r*-NBD2) on the right.

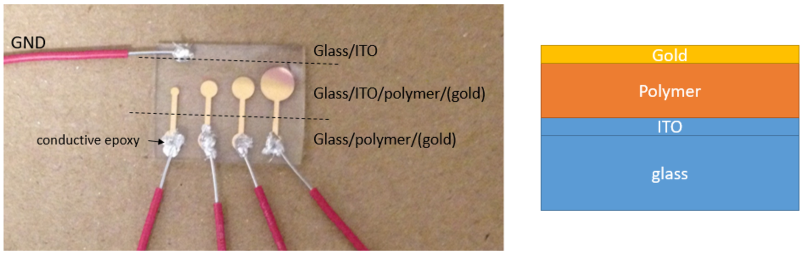

Fig. 6. Picture and side view depiction of the sample to determine dielectric constants.

3.2. Dielectric constants

The dielectric properties of CHIPs films were also measured to interrogate the electrical stability of poly(S-*r*-DIB) thin films when subjected to external fields, as is often required for poling, or other morphological ordering methods. Thin films of poly(S-*r*-DIB) (50-wt% and 70-wt% copolymers) were deposited by spin-coating onto ITO-coated glass slides with the ITO layer etched away on half of the glass substrate. Once thin films are made as described in Section 2.2, gold electrodes are deposited using sputtering through a shadow mask. The electrode pattern is shown below in Fig. 6. The pads with varying area are deposited on the half of the substrate with an ITO layer remaining so as to create a parallel plate capacitor between the ITO and the gold electrode, with the sulfur polymer material between capacitor plates. Wire leads are attached with conductive epoxy on the constant size pads and on the opposite side as a ground.

The values of area A, thickness d, and capacitance C, are measured with an optical microscope, profilometer, and LCR meter, respectively. The capacitor relationship is shown in (2), where ϵ_0 is the constant for vacuum permittivity. The only unknown is the dielectric constant ϵ_r.

$$C = \frac{A\epsilon_0\epsilon_r}{d} \rightarrow \epsilon_r = C\left(\frac{d}{A\epsilon_0}\right) \tag{2}$$

The equation can be rearranged as shown to solve for the dielectric constant ϵ_r in terms of known and measured values. Then the results can be plotted so that the slope of the linear fitted line represents the dielectric constant. An example of this method is shown for 50/50 SDIB in Fig. 7.

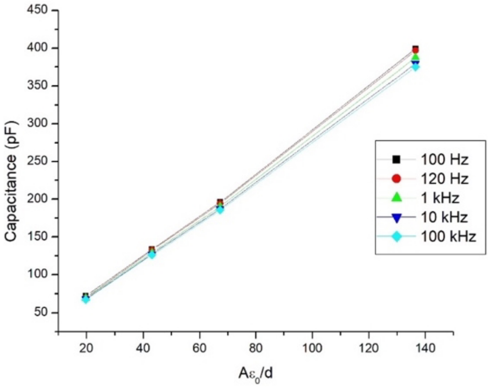

Fig. 7. Plot for poly(S-*r*-DIB) (50-wt%) of the capacitance measured with an LCR meter vs. the calculated value Aε_0/d. Each line represents a different frequency, and each point on a line represents a different electrode area.

The dielectric constant results for poly(S-*r*-DIB) copolymers with compositions of 50/50 and 70/30 weight ratios are shown in Table 1.

Table 1. Calculated values of dielectric constant ϵ_r for poly(S-r-DIB) thin films.

Polymer	Thickness (μm)	100 Hz	120 Hz	1 kHz	10 kHz	100 kHz
S-*r*-DIB 50/50	2.25	2.814	2.805	2.735	2.678	2.641
S-*r*-DIB 70/30	1.22	3.107	3.111	3.038	2.982	2.949

4. Discussion and conclusions

The material characterization done in this work helps to expand the basic knowledge of these important new hybrid materials which are finding applications in infrared imaging, 3D sensing, and integrated photonics, among other areas. For the first time ellipsometry measurements were performed on the CHIPs materials poly(S-*r*-DIB) and poly(S-*r*-NBD_2) from 500 nm to 12 **μ**m, showing that high refractive indices are maintained over this region with relatively low refractive index dispersion except near strong absorption resonances. We show that in the technologically important SWIR region of the optical spectrum, both polymers have high SWIR Abbe numbers (>130), with values in excess of those for the common optical polymer polycarbonate for both 50/50 and 70/30 poly(S-*r*-NBD_2). We can see by inspection of the Figs. 3,4 and 5 that poly(S-*r*-NBD_2) has a much simpler refractive index dispersion and larger windows of transparency in the MWIR than poly(S-*r*-DIB); this is a direct result of the simpler molecular structure of NBD_2 compared to DIB.

The dielectric constant measurements add to our understanding of the molecular interactions within these thin films. While there is a direct relationship between dielectric constant and refractive index, there are other factors that contribute to the relationship. By studying the refractive index and the dielectric constant together, we can get a better understanding of a materials overall electromagnetic response. The dielectric constant at low frequencies is practically equal to the square of the refractive index; for example for S-*r*-DIB, the square of *n* for a wavelength of 4μm is 2.89, while the low frequency dielectric constant is 2.8. This indicates that there are no strong low frequency modes of dielectric excitation in CHIPs polymers and that the optical and electrical properties derive largely from the high atomic polarizability of sulfur.

In summary, CHIPs have a combination of optical and electrical properties that are promising for commercial applications in the IR. In the future, the processing of these films can be improved, especially in the area of micro and nanofabrication. In this way they can then be more readily incorporated onto existing optoelectronic platforms, such as silicon.

Funding. National Science Foundation (CHE-2201155, DMREF-2118578, MRI-1920234, PFI-RP 1940942); Air Force Research Laboratory (FA8650-16-D-5404); National Research Foundation of Korea (2021R1A2C2006167); RII Research Advancement Program.

Acknowledgement. We acknowledge the assistance of Woolam Inc. in performing the ellipsometry measurements.

Disclosures. RAN (I,E) R. A. Norwood is an owner and officer of Norcon Technologies Holding Inc. with which a financial conflict of interest exists.

Data availability. Data underlying the results presented in this paper are not publicly available at this time but may be obtained from the authors upon reasonable request.

References

1. T. S. Kleine, R. S. Glass, D. L. Lichtenberger, M. E. Mackay, K. Char, R. A. Norwood, and J. Pyun, "100th Anniversary of Macromolecular Science Viewpoint: High refractive index polymers with elemental sulfur for infrared thermal imaging and optics," ACS Macro Lett. **9**(2), 245–259 (2020).
2. W. J. Chung, J. J. Griebel, E. T. Kim, H. Yoon, A. G. Simmonds, H. J. Ji, P. T. Dirlam, R. S. Glass, J. J. Wie, N. A. Nguyen, B. W. Guralnick, J. Park, A. Somogyi, P. Theato, M. E. Mackay, Y.-E. Sung, K. Char, and J. Pyun, "The use of elemental sulfur as an alternative feedstock for polymeric materials," Nat. Chem. **5**(6), 518–524 (2013).

3. J. Griebel, S. Namnabat, E. T. Kim, R. Himmelhuber, D. Moranta, W. J. Chung, A. G. Simmonds, K.-J. Kim, J. van der Laan, N. A. Nguyen, E. L. Dereniak, M. E. Mackay, K. Char, R. S. Glass, R. A. Norwood, and J. Pyun, "New infrared transmitting material via inverse vulcanization of elemental sulfur to prepare high refractive index polymer," Adv. Mater. **26**(19), 3014–3018 (2014).
4. L. E. Anderson, T. S. Kleine, Y. Zhang, D. D. Phan, S. Namnabat, E. A. LaVilla, K. M. Konopka, L. Ruiz Diaz, M. S. Manchester, J. Schwiegerling, R. S. Glass, M. E. Mackay, K. Char, R. A. Norwood, and J. Pyun, "Chalcogenide hybrid inorganic/organic polymers: Ultrahigh refractive index polymers for infrared imaging," ACS Macro Lett. **6**(5), 500–504 (2017).
5. A. Nishant, K.-J. Kim, S. Showghi, R. Himmelhuber, T. Kleine, T. Lee, J. Pyun, and R. A. Norwood, "High refractive index chalcogenide hybrid inorganic/organic polymers for integrated photonics," Adv. Opt. Mater. **2022**, 2200176 (2022).
6. T. S. Kleine, T. Lee, K. J. Carothers, M. O. Hamilton, L. E. Anderson, L Ruiz Diaz, N. P. Lyons, K. R. Coasey, W. O. Parker Jr., L. Borghi, M. E. Mackay, K. Char, R. S. Glass, D. L. Lichtenberger, R. A. Norwood, and J. Pyun, "Infrared fingerprint engineering: A molecular design approach to long-wave infared transparency with polymeric materials," Angew. Chem. **131**, 17820–17824 (2019).
7. J. N. Hilfiker and T. Tiwald, "Dielectric Function Modeling," Chapter 5 in *Spectroscopic Ellipsometry for Photovoltaics*, H. Fujiwara and R. W. Collins, (Springer, 2019).
8. W. Groh, "Overtone absorption in macromolecules for polymer optical fibers," Makromol. Chem. **189**(12), 2861–2874 (1988).
9. G. Beadie, M. Brindza, R. A. Flynn, A. Rosenberg, and J. S. Shirk, "Refractive index measurements of poly(methyl methacrylate) (PMMA) from 0.4-1.6 µm," Appl. Opt. **54**(31), F139–F143 (2015).
10. X. Zhang, J. Qiu, X. Li, J. Zhao, and L. Liu, "Complex refractive indices measurements of polymers in visible and near-infrared bands," Appl. Opt. **59**(8), 2337–2344 (2020).